Solving an internal problem
for finite regular two-dimensional lattice spiral
elements, excitable plate electromagnetic wave

Dmitry P. Tabakov[1] (iD)*, Bassam Mohammed-Ali Al-Nozaili*[2]

[1] Povolzhskiy State University of Telecommunications and Informatics
23, L. Tolstoy Street,
Samara, 443010, Russia
[2] Samara National Research University
34, Moskovskoye shosse,
Samara, 443086, Russia

Abstract – **Background.** The work is aimed at developing and researching rigorous methods for solving internal problem of electrodynamics for multi-element structures (metastructures) consisting from the final number of elements, as well as to study the physical processes occurring in them. A special case of such structures are two-dimensional lattices with a fixed interelement distance, consisting of identical elements having the same spatial orientation (regular lattices). **Aim.** In this work, based on an iterative approach, the internal solution is solved. problems of electrodynamics for a finite regular two-dimensional lattice of spiral elements. In order to obtain a priori information about the electrodynamic characteristics of elements lattice and justification for the choice of projection function systems are analyzed spectral characteristics of the integral operator of the internal problem for a single spiral element. Then the currents on the structure elements are calculated, their spectral characteristics are determined. The results of spectral analysis allow increase the efficiency of solving an internal problem. **Methods.** The research is based on a strict electrodynamic approach, within the framework of which, for the specified structure in the thin-wire approximation, an integral representation of the electromagnetic field is formed, which, when considered on the surface of conductors together with boundary conditions, is reduced to a system of Fredholm integral equations of the second kind, written relative to unknown current distributions on conductors (internal task). The solution of the internal problem within the framework of the method of moments is reduced to solving a SLAE with a block matrix. **Results.** A mathematical model of a finite two-dimensional lattice of spiral elements is proposed radiating structure. For the specified structure, in the case of its excitation by a flat electromagnetic wave, based on the iterative approach, the internal problem of electrodynamics was solved. The following were carried out in a wide frequency range: analysis of the convergence of the iterative process, spectral analysis of the integral operator of the internal problem for a single spiral element, as well as spectral analysis of external field and current functions functions on lattice elements. **Conclusion.** The feasibility of determining the spectral characteristics of integral operators is shown internal task for the elements forming the metastructure. A relationship has been identified between the frequency dependence eigenvalues of the integral operator of the internal problem of single elements, forming a metastructure, with resonance phenomena arising in the metastructure, the influence of resonances on the convergence of the iterative process was confirmed. The feasibility of considering averaged amplitude current spectra is shown. It was revealed that the averaged spectrum of current functions is close to degenerate, especially near resonant frequencies. This allows for use as projection functions a compact set of eigenfunctions that have significant amplitudes in the vicinity of the frequency under study, which significantly simplifies the solution of the internal problem.

Keywords – metastructure; spiral structure; Fredholm integral equation; thine-wire approximation; integral representation of the electromagnetic field; resonance; current distribution; Gauss–Seidel method; eigenfunction method.

Introduction

One of the principal trends in electrodynamics is the study of processes in emitting and re-emitting antenna arrays and the determination of the properties of generated and dissipated electromagnetic fields (EMFs). The former is known as the emitting problem, whereas the latter is the EMF diffraction problem. The study of the processes in such arrays requires identifying current distribution functions over array components. This is the internal electrodynamic problem. Meanwhile, the external electrodynamic problem involves the determination of the proper-ties of the EMF generated by the current. The above problems are general by nature.

Note that an array is any structure containing multiple components. Each component has its current distribution function. The vast majority of real-world antennas (e.g., phased antenna arrays) fall under this definition. Re-emitting arrays include chiral structures [1], photonic crystals [2], diffraction gratings, some types of microwave lenses and slow-wave circuits, and any microstructures. The above-listed examples, except for microstructures, are called metastructures or metamaterials. Metamaterials are manufactured by introducing particles of various

shapes into a base material to modify its dielectric and magnetic susceptibility. They consist of repeating patterns that govern their properties. The paper by V.G. Veselago [3] can be considered the foundation of metamaterials science. Metamaterials can have unconventional properties not found in natural materials, such as their negative refractive index [4] (left-handed materials). D.R. Smith and his team at the University of California, San Diego [5] reinvented and demonstrated such materials more than 30 years after V.G. Veselago published his article. Their work was based on the study by J.B. Pendry [6–8].

Nowadays, metamaterials are used in high-performance microwave devices and antenna feeders. The review of Vendik et al. [9] presented the applications of metamaterials to microwave devices and antennas. Other examples of metamaterials are photonic crystals [2]. They can be used to make optical filters, waveguides, and many other devices.

Interactions between elements in emitting and re-emitting arrays are of special interest. These interactions must be incorporated into valid mathematical models of antenna arrays. A valid mathematical model correctly represents the processes in an array. Meanwhile, an effective mathematical model significantly reduces the time and resources required to analyze or design an array with specified characteristics.

Throughout the development of electrodynamics, optics, and microwave device technology, numerous methods, each with distinct advantages and disadvantages, have been developed. Among these, the induced EMF method has been used for a long time to analyze interactions in multielement emitting arrays. Schelkunoff et al. [10] presented the basic principles of this method. Using the induced EMF method, one can find the affected impedances of antenna elements and the amplitudes and phases of currents in passive antenna elements. However, a disadvantage of this method involves some restrictions on the length and distance between array elements as approximate current distributions are used.

Nowadays, computer-aided design (CAD) systems are used to solve such problems using the method of moments [11], the finite element method, and the finite difference method [12]. However, the drawbacks of this approach include the high requirements for computer hardware performance, expensive soft-

ware, and the unavailability of an explicit mathematical model of the analyzed antenna array.

CAD systems can also be used for the analysis of metamaterials with the pros and cons already mentioned. Rigorous methods with periodic boundary conditions are the most efficient options for the analysis of metamaterials with a regular structure pattern used in long- or unlimited-wavelength antenna arrays. Meanwhile, simplified approaches use circuit theory methods (equivalent circuits) and effective dielectric and magnetic permeability. Optical and quasioptical methods are also suitable for the analysis of metamaterial antenna arrays working with long wavelengths. In this respect, the validity of any simplified model should always be confirmed [13].

Therefore, general-purpose methods must be developed for the analysis of interelement interactions in antenna arrays. In this regard, Ilinskiy et al. [14] proposed an iterative approach to solving integral equations used in the wire antenna theory. The approach was based on the multistep minimal residual method. This method was applied directly to the general matrix of a system of linear algebraic equations (SLAE). Meanwhile, Neganov et al. [15] used a modification of the Gauss–Seidel method [16] for a block matrix of an SLAE for interaction analysis. The method was applied to solve a diffraction problem for a metastructure, a thin layer with finite dimensions consisting of double open rings. The proposed method was found to be effective for the analysis of metastructures with finite dimensions. Further, Neganov et al. [17] considered the problem of a plane electromagnetic wave (PEMW) diffraction on a chiral layer. The layer was a rectangular, evenly spaced 10 × 10 array composed of five-segment S-elements. They showed that despite the rather small number of chaotically oriented S-elements, the scattering diagrams were quite oriented. In another study [18], the findings presented by Neganov et al. [15] were supplemented with algorithms for the calculation of the SLAE block matrix elements for a structure consisting of identical elements with different types of symmetry. These algorithms significantly reduced the computation time. Tabakov et al. [19] considered the applicability of the method presented by Neganov et al. [15] to the analysis of current distributions in a director antenna [20]. The method had good convergence for the analysis of a director antenna in a specified frequency range.

Further, Tabakov et al. [21] studied the applicability of the iterative approach to solving the internal problem for a symmetrical vibrator with a reflector made of parallel rectilinear conductors. They also presented a key algorithm for calculating the block matrix elements. The algorithm's running time increased linearly with the number of reflector elements. The authors also provided recommendations on the selection of projection function systems (PFSs) depending on the symmetries present in the structure. They also studied the distributions of the currents, input resistance, and radiation characteristics of the structure.

This study aimed to solve the internal problem for a finite regular two-dimensional (2D) array consisting of conical spiral elements. The array was excited by a plane linearly polarized electromagnetic wave. We used the method proposed by Neganov et al. [15] as a basis for the solution of the internal problem. We also proposed an algorithm for calculating the compact block matrix based on the algorithms described previously [18]. We performed a spectral analysis of the internal problem's integral operator for a single spiral element as previously described [22] because the resonance properties of the array elements affect the convergence of the iterative process. Another reason was to verify the selection of the system of projection functions used in the method of moments. In this paper, we present the following:

– the spectral analysis results for a single spiral element and an array of such elements,

– the convergence of the internal problem solution for an array of elements,

– interpretation of the results, and

– proposals for subsequent research.

1. Basic mathematical expressions

The basic expressions have been sufficiently presented previously [21], but we provide them with some explanation. Let us consider an emitting or reemitting array consisting of the elements v_n ($n \in \mathcal{N}$: $1\ldots N$, N is the number of elements). The array is formed from its unique elements $\underline{v}_u$ by their parallel translation and/or rotation ($u \in \mathcal{U}$: $1\ldots U$, U is the number of unique elements). The internal electrodynamics problem for this array is reduced to the following operator system [19]:

$$\sum_{n'} \Psi_{n,n'}(\eta_{n'}) = \zeta_n, \quad n' \in \mathcal{N}. \tag{1}$$

In this system, $\Psi_{n,n'}$, $n \neq n'$ are operators representing the interaction between the elements v_n and $v_{n'}$; $\Psi_{n,n} = \Psi_n$ is the eigenoperator of the element v_n; ζ_n represents the functions for the currents induced by external fields; and $\eta_{n'}$ indicates the current distribution functions to be defined. The method of moments [11] is applied to system (1). Using the systems of basis $\{\beta\}_{n'} \equiv \{\beta_{q'}\}_{n'}$ and test $\{\tau\}_n \equiv \{\tau_q\}_n$ functions ($q = q_n \in \mathcal{Q}$: $1\ldots Q$, $q' = q_{n'} \in \mathcal{Q'}$: $1\ldots Q'$), we find the scalar product operator of the functions. The sought functions $\eta_{n'}$ are approximated by the following series:

$$\eta_{n'} = \sum_{q'} I_{q'}^{(n')} \beta_{n',q'}. \tag{2}$$

The following SLAE is constructed with respect to the unknown coefficients $I_{q'}^{(n')}$:

$$\overline{\mathbf{Z}}\mathbf{I} = \mathbf{E}, \tag{3}$$

where $\overline{\mathbf{Z}}$ is the block matrix of generalized impedances and $\mathbf{I}$ and $\mathbf{E}$ are the block vectors of the unknowns and the right-hand side, respectively:

$$\overline{\mathbf{Z}} \supset \overline{\mathbf{z}}_{n,n'} \supset Z_{q,q'}^{(n,n')} = <\tau_{n,q}, \Psi_{n,n'}(\beta_{n',q'})>,$$

$$\mathbf{I} \supset \mathbf{i}_{n'} \supset I_{q'}^{(n')}, \quad \mathbf{E} \supset \mathbf{e}_n \supset E_q^{(n)} = <\tau_{n,q}, \zeta_n>.$$

The block matrix elements with identical indices $\overline{\mathbf{z}}_{n,n} = \overline{\mathbf{z}}_n$ form intrinsic impedance matrices, whereas the elements with different indices form mutual impedance matrices. The latter defines the interactions between the metastructure elements. The «<>» brackets denote a scalar product. Let us introduce an array of unique matrices $\{\underline{\overline{\mathbf{z}}}_k\} \equiv \{\underline{\overline{\mathbf{z}}}\}$ ($k \in \mathcal{K}$: $1\ldots U\ldots K$). We assume that the first U matrices of the array $\{\underline{\overline{\mathbf{z}}}\}$ form intrinsic impedance matrices containing unique elements $\underline{v}_u$, whereas the remaining $K-U$ elements form mutual impedance matrices. The array $\{p_{n,n'}^{(\overline{\mathbf{z}})}\}$ with its elements $p_{n,n'}^{(\overline{\mathbf{z}})} = k$ matches the pair of indices $n, n' \in \mathcal{N}$ and the index $k \in \mathcal{K}$. Therefore,

$$\overline{\mathbf{z}}_{n,n'} = \underline{\overline{\mathbf{z}}}_k, \quad k = p_{n,n'}^{(\overline{\mathbf{z}})} \in \{p_{n,n'}^{(\overline{\mathbf{z}})}\} \equiv \{p^{(\overline{\mathbf{z}})}\}.$$

In the general case, the antenna array consists of chaotically arranged, heterogeneous elements v_n. The introduction of the arrays $\{\underline{\overline{\mathbf{z}}}\}$ and $\{p^{(\overline{\mathbf{z}})}\}$ makes no sense as they only insignificantly increase the requirements for computer memory and time. However, when the antenna array contains identical and regularly arranged elements, the inequality $K < N^2$ takes place and the introduction of these arrays makes sense. They contain the fundamental part of the a priori information about the antenna array.

The algorithm for calculating the array of unique matrices is discussed below.

The final stage of the solution for the internal problem is the solution of the block SLAE (3). In this case, matrix-splitting iterative methods [16] seem promising, but if the matrix $\overline{\mathbf{Z}}$ is not diagonally dominant, such methods do not ensure convergence.

To ensure the convergence of classical iterative methods, we can consider the block SLAE (3) assuming that there is no strong relation between the elements. Another factor that greatly affects such convergence is the selection of PFSs. The optimal option is the systems of eigenfunctions (EFs) of the elements or a PFS closely similar to the EFs [23]. The EF computation is an auxiliary problem. Its complexity is determined by the number of unique elements $\underline{v}_u$ and their properties. The complete eigenvalue (EV) problem for the intrinsic impedance matrices of unique elements $\overline{\mathbf{z}}_u$, obtained using the method of moments, basis functions $\beta_{u,q}$, and test functions $\tau_{u,q}$, is expressed as follows:

$$\overline{\mathbf{z}}_u \overline{\mathbf{J}}^{(u)} = \mathcal{D}(\mathbf{x}^{(u)})\overline{\mathbf{J}}^{(u)},$$

where $\overline{\mathbf{J}}^{(u)}$ is a matrix whose columns contain eigenvectors (EVEC) of the matrix $\overline{\mathbf{z}}_u$; $\mathcal{D}(\mathbf{x}^{(u)})$ is the diagonal matrix formed by the vector $\mathbf{x}^{(u)}$, whose elements ξ_q are the corresponding EVs of the matrix $\overline{\mathbf{z}}_u$; and $\mathcal{D}$ is the operator that produces the diagonal matrix. The operand $\mathcal{D}$ is a vector of the main diagonal elements or a matrix whose main diagonal elements are used by the operator $\mathcal{D}$ to create the diagonal matrix. From here onward, we assume that complex matrices $\overline{\mathbf{z}}_u$ are symmetrical for single elements. The EV ξ_q approximates the EVs of the integral operators $\underline{\Psi}_u$, whereas the EFs of the above integral operators are approximated by the EVECs as follows:

$$\breve{\beta}_{u,q} \approx \sum_{q'=1}^{Q'} J_{q',q}^{(u)} \beta_{u,q'}, \quad J_{n,q}^{(u)} \in \overline{\mathbf{J}}^{(u)}.$$

In the following, this problem is considered for a conical spiral element of the antenna array.

Applying the Gauss–Seidel procedure [16] to the block SLAE, we obtain the following solution:

$$\mathbf{i}_n^{(l+1)} = \overline{\mathbf{p}}_n \mathbf{e}_n - \sum_{l>i} \overline{\mathbf{w}}_{n,n'} \mathbf{i}_{n'}^{(l)} - \sum_{l<i} \overline{\mathbf{w}}_{n,n'} \mathbf{i}_{n'}^{(l+1)}, \tag{4}$$

l hereinafter is the current iteration step:

$$\overline{\mathbf{p}}_n = \overline{\mathbf{z}}_{n,n}^{-1}, \quad \overline{\mathbf{w}}_{n,n'} = \overline{\mathbf{p}}_n \overline{\mathbf{z}}_{n,n'},$$

where $\overline{\mathbf{p}}_n$ represents inverse eigenmatrices and weight matrices, respectively, and it acts as the preconditioner matrices. Procedure (4) can also use a simpler option:

$$\overline{\mathbf{p}}_n = \mathcal{D}(\overline{\mathbf{z}}_{n,n})^{-1}.$$

If we assume that the second sum (4) $l+1=l$, then the equation represents the simple iteration method. The convergence criterion is the following inequality:

$$\delta_l = \max_n (|\mathbf{i}_n^{(l+1)} - \mathbf{i}_n^{(l)}| / |\mathbf{i}_n^{(l+1)}|) \le \delta_*, \tag{5}$$

where δ_* is an arbitrarily small predetermined number. Hereinafter, $|\mathbf{v}|$ is the Euclidean norm of the vector $\mathbf{v}$.

2. Integral representations of the EMF in a thin-wire multielement array

The multielement thin-wire array L is a set of N thin conductors L_1, L_2, …, L_N of arbitrary shape arranged in a free space with the wave impedance W_m. For simplicity, let us assume that all the conductors have the same radius ε. Each conductor can be described by a vector equation as a function of the natural parameter l:

$$\mathbf{r}_n(l) = \hat{\mathbf{x}}X_n(l) + \hat{\mathbf{y}}Y_n(l) + \hat{\mathbf{z}}Z_n(l), \quad l \in [L_{n,\min}, L_{n,\max}],$$

where $X_n(l)$, $Y_n(l)$, and $Z_n(l)$ are smooth functions. The length of the nth conductor is $L_n = L_{n,\max} - L_{n,\min}$. The integral representation of the EMF (IR EMF) of such an array can be expressed as follows [24]:

$$\mathbf{F}(\mathbf{r}) = \sum_{n'=1}^{N} \int_{L_{n'}} I_{n'}(l') \mathbf{K}^{(F)}(\mathbf{r}, \mathbf{r}_{n'}(l')) dl', \quad F \equiv E, H; \tag{6}$$

where $I_{n'}(l')$ is the total current distribution along the generatrix $L_{n'}$.

$$\mathbf{K}^{(E)} = \frac{W_m}{ik}\left[k^2 \hat{\mathbf{l}}' G dl - \frac{\partial}{\partial l}\left((\mathbf{r} - \mathbf{r}')B\right)\right],$$

$$\mathbf{K}^{(H)} = \hat{\mathbf{l}}' \times (\mathbf{r} - \mathbf{r}')B$$

are the IR EMF cores, $\mathbf{r}' = \mathbf{r}_{n'}(l')$ is the vector equation of the generatrix $L_{n'}$, and $\hat{\mathbf{l}}' = \hat{\mathbf{l}}_{n'}(l') = d\mathbf{r}_{n'}(l')/dl'$ is the unit vector of the tangent defined at point l' on the generatrix $l_{n'}$.

$$G = \frac{\exp(-ikR)}{4\pi R}, \quad B = \frac{1}{R}\frac{\partial G}{\partial R} = -\frac{ikR+1}{R^2}G,$$

$$R = \sqrt{|\mathbf{r} - \mathbf{r}'|^2 + \varepsilon^2}$$

are Green's functions for free space and its derivative, respectively, and R is the distance regularized by the conductor radius ε.

$I_{n'}(l')$ can be reasonably represented by series (2). Then, the initial IR EMF (6) is

$$\mathbf{F}(\mathbf{r}) = \sum_{n'}\sum_{q'} I_{q'}^{(n')} \int_{L_{n'}} \beta_{n',q'}(l') \mathbf{K}^{(F)}(\mathbf{r},\mathbf{r}_{n'}(l'))dl', \quad F \equiv E,H;$$

The boundary condition for an ideal conductor is valid for each generatrix:

$$(\mathbf{E}^{((in))}(\mathbf{r}_n(l)) + \mathbf{E}(\mathbf{r}_n(l))) \cdot \hat{\mathbf{l}}_n(l) = 0. \tag{7}$$

Multiplying (7) alternately with the test functions $\tau_{n,q}(l)$ and integrating over l, we obtain an SLAE for computing $I_{q'}^{(n')}$, which is similar to (3), where

$$Z_{q,q'}^{(n,n')} = \int_{L_n}\int_{L_{n'}} \tau_{n,q}(l)\beta_{n',q'}(l')\mu^{(n,n')}(l,l')dl'dl, \tag{8}$$

$$E_q^{(n)} = \int_{L_n} \tau_{n,q}(l)\nu^{(n)}(l)dl;$$

$$\mu^{(n,n')}(l,l') = \hat{\mathbf{l}}_n(l) \cdot \mathbf{K}^{(E)}(\mathbf{r}_n(l),\mathbf{r}_{n'}(l')),$$

$$\nu^{(n)}(l) = \hat{\mathbf{l}}_n(l) \cdot \mathbf{E}^{((in))}(\mathbf{r}_n(l)).$$

Let us describe the calculation of the integrals in (8) using the conductor segmentation procedure. In this procedure, the nth conductor is represented as a set of $M+1$ nodes $L_n^{(M)}$: $\mathbf{r}_{n,1}$, $\mathbf{r}_{n,2}$, …, $\mathbf{r}_{n,M+1}$. The mth segment $\mathbf{r}_{n,m}(l)$, is located between the nodes with numbers m and $m+1$, represented as

$$\mathbf{r}_{n,m}(l) = \dot{\mathbf{r}}_{n,m} + \hat{\mathbf{l}}_{n,m}l, \quad l \in [-\Delta_{n,m}/2, \Delta_{n,m}/2],$$

where $\dot{\mathbf{r}}_{n,m} = (\mathbf{r}_{n,m} + \mathbf{r}_{n,m+1})/2$ is the center of the segment, $\Delta_{n,m} = |\mathbf{r}_{n,m+1} - \mathbf{r}_{n,m}|$ is the segment length, and $\hat{\mathbf{l}}_{n,m} = (\mathbf{r}_{n,m+1} - \mathbf{r}_{n,m})/\Delta_{n,m}$ is the unit vector of the tangent to the segment. Hereinafter, the indices $m \in \mathcal{M}$: $1...M$ and $m' \in \mathcal{M'}$: $1...M'$ are associated with the segments of the nth and n'^{th} elements of the array, respectively.

We use the weighted sums of functions that are piecewise constants within each segment as basic functions:

$$\beta_{n,q}^{(M)}(l) = \sum_m \beta_{n,q}(\dot{l}_{n,m})\sigma(l',\dot{l}_{n,m},\Delta_{n,m}), \tag{9}$$

where $\dot{l}_{n,m}$ is the value of the natural parameter on the segmented generatrix $L_n^{(M)}$ at the center of the segment with index m and $\sigma(l,\dot{l},\Delta)$ is the function describing a rectangular unit pulse with its center at point $\dot{l}$ and width Δ. We use weighted sums of the Dirac delta functions as test functions:

$$\tau_{n,q}^{(M)}(l) = \sum_m \tau_{n,q}(\dot{l}_{n,m})\delta(l - \dot{l}_{n,m}). \tag{10}$$

This approach can be considered as a generalized collocation method [25]. The expressions above show that in case (9), the values of the functions $\beta_{n,q}(l)$, calculated at the collocation points $\dot{l}_{n,m}$, act as weighting coefficients, whereas these are the functions $\tau_{n,q}(l)$ in case (10).

From expression (8) and considering delta function properties, we obtain equations for the SLAE matrix coefficients and right-hand side coefficients using the following finite sums:

$$Z_{q,q'}^{(n,n')} \approx \sum_m\sum_{m'} \tau_{n,q}(\dot{l}_{n,m})\beta_{n',q'}(\dot{l}_{n',m'})\mu_{m,m'}^{(n,n')}, \tag{11}$$

$$E_q^{(n)} \approx \sum_m \tau_{n,q}(\dot{l}_{n,m})\nu_m^{(n)},$$

where

$$\mu_{m,m'}^{(n,n')} = \int_{\Delta_{n',m'}} \mu^{(n,n')}(\dot{l}_{n,m},l')dl', \quad \nu_m^{(n)} = \nu^{(n)}(\dot{l}_{n,m}).$$

The conventional collocation method corresponds to

$$\beta_{n,q}(l) = \delta_{l,\dot{l}_{n,q}}, \quad \tau_{n,q}(l) = \delta_{l,\dot{l}_{n,q}},$$

where $\delta_{x,y}$ is the Kronecker delta. A correct solution of the SLAE using the collocation method is achieved when the following condition [26] for any segment is satisfied:

$$2\varepsilon \le \Delta \le 12\varepsilon. \tag{12}$$

3. Antenna array

Fig. 1, *a* shows the arrangement of the studied antenna array, and Fig. 1, *b* shows the geometry of a spiral element. The antenna is a rectangular grid in the plane xOy. with a size of $L_x \times L_y$. The nodes of the grid contain re-emitting elements with identical shapes and spatial orientation. As the grid spacing is constant, the entire array is regular. The size of the re-emitting elements does not exceed D. A PEMW with linear polarization excites the reradiation. The PEMW angle of incidence in the antenna array is arbitrary. The external electric field $\mathbf{E}^{(in)}$ generated by the wave excites currents distributed along the re-emitting elements. These currents induce the EMF generated by the antenna array.

Let us consider the antenna array in detail. For convenience, double indices are used for the array nodes and elements. We denote the indices along the array
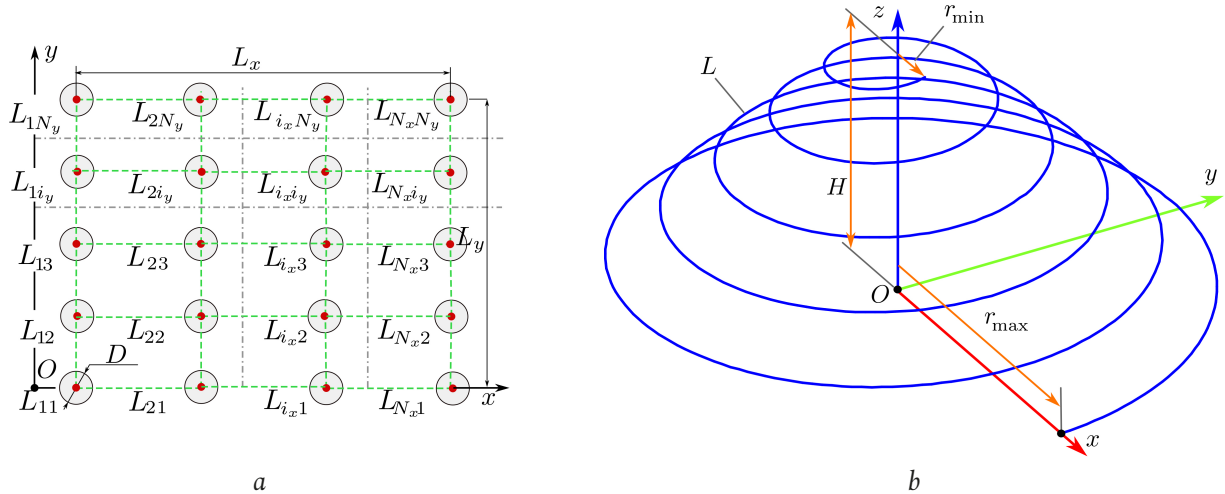
Fig. 1. Antenna array (*a*) and geometry of its elements (*b*)
Рис. 1. Геометрия решетки (*a*) и образующих ее элементов (*б*)

axes i_x, i_y. When filling in the final SLAE matrix, the double to consecutive indices ($n = 1 \ldots N$):

$$n = i_x + (i_y - 1)N_x, \quad i_x = 1, \ldots, N_x, \quad i_y = 1, \ldots, N_y. \quad (13)$$

Let us consider the geometry of the array. Hereinafter, h_x and h_y are the distances between neighboring elements. With these notations, we can find the coordinates of the array nodes:

$$\mathbf{r}_{i_x, i_y} = \hat{\mathbf{x}}(h_x(i_x - 1) - L_x / 2) + \hat{\mathbf{y}}(h_y(i_y - 1) - L_y / 2).$$

N_x and N_y are the numbers of the array elements along the axes. In this case,

$$L_x = (N_x - 1)h_x, \quad L_y = (N_y - 1)h_y.$$

The elements L_{i_x, i_y} of the array are conical spirals made of a perfect conductor with a circular cross-section. The axis of each spiral is parallel to the axis Oz. Fig. 1, *b* shows the spiral element. The minimum radius of the spiral is $r_{\min}$, whereas the maximum radius is $r_{\max}$. The height of the spiral is H, and the number of turns is N_l. The axis of a spiral element is the line coinciding with the axis Oz. The diameter of conductors 2ε is essentially less than λ and essentially less than the size of the spirals and the turn-to-turn distance. Such geometry allows us to use thin-wire approximation in the antenna array model (see the expressions given in the previous section).

The general equation of the conical Archimedean spiral is

$$L : \mathbf{r}(t) = (r_{\max} - h_r t)\cos(st)\,\hat{\mathbf{x}} + \quad (14)$$
$$+ (r_{\max} - h_r t)\sin(st)\,\hat{\mathbf{y}} + h_z t\,\hat{\mathbf{z}},$$
$$t \in [0, 2\pi N_l],$$

where t is a non-natural parameter, $r_{\min}$ and $r_{\max}$ are the minimum and maximum radii of the spiral, re-

spectively, H is the spiral height, N_l is the number of turns, h_r is the radial factor, and h_z is the axial pitch factor. The parameter $s = \pm 1$ specifies the winding direction; thus, the parametric equation can be used to analyze both the left and right spirals. The variables h_r and h_z can be estimated for the given $r_{\min}$, $r_{\max}$, H, and N_l as follows:

$$h_r = \frac{r_{\max} - r_{\min}}{2\pi N_l}, \quad h_z = \frac{H}{2\pi N_l}. \quad (15)$$

To determine the natural parameter of the conic spiral, the following expression is used:

$$l(t) = \int_0^t |\mathbf{l}(t')|\, dt', \quad (16)$$

where $\hat{\mathbf{l}}(t) = d\mathbf{r}(t)/dt$ is the tangent unit vector defined at the point $\mathbf{r}(t)$ of the generatrix. The equation of the conical Archimedean spiral with a natural parameter can be obtained from (14) with the substitution $t \to t(l)$. For the function $t(l)$, there is no explicit expression on the conical Archimedean spiral, so it can only be found numerically using expression (16) and the inverse interpolation method [16]. Any element L_{i_x, i_y} of the array can be obtained as

$$L_{i_x, i_y} : \mathbf{r}_{i_x, i_y}(l) = \overline{\mathbf{R}}^{(z)}(\phi_{i_x, i_y})\mathbf{r}(l) + \mathbf{r}_{i_x, i_y}, \quad (17)$$

where $\overline{\mathbf{R}}^{(z)}(\phi)$ is the rotation around the axis Oz by the angle ϕ. Now, we can switch to consecutive numbering (13) and use the expressions given in the previous section.

The PEMW field W (Fig. 2) is as follows:

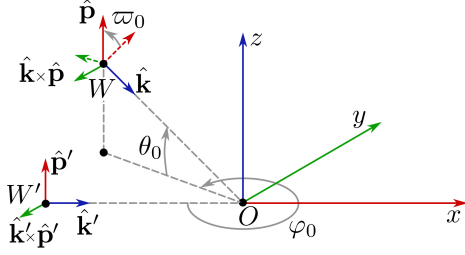$$\mathbf{E}^{(in)}(\mathbf{r}) = \hat{\mathbf{p}} E_0 \exp(-i\mathbf{k}\mathbf{r} + \psi_0), \quad (18)$$

Fig. 2. PEMW W against the primary wave W' and the global Cartesian coordinate system

Рис. 2. Связь плоской электромагнитной волны W с первичной волной W' и глобальной декартовой системой координат

$$\mathbf{H}^{(\mathrm{in})}(\mathbf{r}) = [\hat{\mathbf{k}} \times \hat{\mathbf{p}}]\frac{E_0}{W_m}\exp(-i\mathbf{kr} + \psi_0),$$

where $\mathbf{k} = \hat{\mathbf{k}}k$, $\hat{\mathbf{k}}$ is the wave unit vector, k is the wave number, E_0 is the amplitude of the electric field vector, W_m is the wave (characteristic) impedance of the medium, ψ_0 is the initial phase of the wave, and $\hat{\mathbf{p}}$ is the polarization vector that specifies the oscillation direction of the wave vector $\mathbf{E}$.

PEMW is defined by five parameters: amplitude E_0, phase ψ_0, polarization angle ϖ_0, and two angles θ_0 and φ_0 that specify the direction of wave propagation. Let us define the base wave W' (Fig. 2). Its unit vectors $\hat{\mathbf{k}}'$, $\hat{\mathbf{p}}'$ coincide with the axes of the global rectangular coordinate system. To avoid ambiguity, we assume that $\hat{\mathbf{p}}' = \hat{\mathbf{z}}$, $\hat{\mathbf{k}}' = \hat{\mathbf{x}}$. In this way, the wave W' has a vertical polarization and propagates along the axis Ox. The relationship between the unit vectors of the waves W and W' is

$$\mathbf{v} = \overline{\mathbf{R}}^{(z)}(\varphi_0)\overline{\mathbf{R}}^{(y)}(\theta_0)\overline{\mathbf{R}}^{(x)}(\varpi_0)\mathbf{v}', \quad \mathbf{v} \equiv \hat{\mathbf{p}}, \hat{\mathbf{k}}.$$

In this expression, $\overline{\mathbf{R}}^{(f)}(\phi)$ represents the matrices of rotation around the axes and ϕ is the rotation angle; $f \equiv x, y, z$.

4. Obtaining the array of unique matrices

A previous study [18] presented direct and key-based algorithms for calculating $\{p^{(\overline{\mathbf{z}})}\}$ and $\{\underline{\mathbf{z}}\}$. These algorithms could be either exact or approximate. The advantage of the direct algorithm was its versatility, whereas the main disadvantage was the higher computational complexity due to the comparison of the blocks of the matrix $\overline{\mathbf{Z}}$. However, this previous study [18] did not indicate that such an approach could be effective for analyses with multiple frequencies and/or large numbers of antenna array excitation options because the algorithm is not iterative. To estimate

the array of unique matrices for the considered antenna array, we propose an approximate combined algorithm. The informative parameters $\iota_{n'}$, ι_n are truncated systems of the basis $\{\tilde{\beta}\}_{n'} \equiv \{\beta_{\tilde{q}'}\}_{n'}$ and test $\{\tilde{\tau}\}_n \equiv \{\tau_{\tilde{q}}\}_n$ functions ($\tilde{q} = \tilde{q}_n \in \tilde{\mathcal{Q}}$: $1...\tilde{Q}$, $\tilde{q}' = \tilde{q}_{n'} \in \tilde{\mathcal{Q}}'$: $1...\tilde{Q}'$; $\tilde{Q} \ll Q$, $\tilde{Q}' \ll Q'$). In this case, the keys $\kappa = \kappa(\iota_n, \iota_{n'})$ are matrices of intrinsic and mutual impedances of small dimensionality $\tilde{\mathbf{z}}_{n,n'} = \langle \tau_{n,\tilde{q}}, \Psi_{n,n'}(\beta_{n',\tilde{q}'}) \rangle$. For the considered antenna array, the truncated PFSs can be derived from the following systems of functions:

$$\beta_{n,q}(l) = \sqrt{2}\cos((2q-1)\pi l/(2L)), \quad \tau_{n,q}(l) = \beta_{n,q}(l). \quad (19)$$

These systems are quite similar to the EF system for a thin rectilinear conductor of length L at small values of L/λ [23]. For the given antenna array, the generalized collocation method can be used to obtain $\tilde{\mathbf{z}}_{n,n'}$ using expressions (9)–(11).

The algorithm steps are as follows:

• The key $\kappa = \kappa(\iota_n, \iota_{n'})$; is calculated for the current n, n' from the informative parameters ι_i, ι_j of the current elements.

• The key κ' is sought in $\{\underline{\kappa}\}$, to satisfy the condition $\rho = |\kappa - \kappa'|/|\kappa'| \le \rho_*$, where ρ_* is the acceptable key mismatch.

• If the key κ' in the kth position of the vector $\{\underline{\kappa}\}$, satisfies the condition $\rho \le \rho_*$, then $p_{n,n'}^{(\overline{\mathbf{z}})} = k$.

• If no key $\kappa' \in \{\underline{\kappa}\}$ satisfies the condition $\rho \le \rho_*$, then the key κ, is added to the vector $\{\underline{\kappa}\}$ and the matrix $\overline{\mathbf{z}}_{n,n'}$ is added to the vector $\{\underline{\mathbf{z}}\}$, where K' is the number of elements of the expanded vector $\{\underline{\kappa}\}$.

The algorithm is performed first for matching and then for mismatching n and n'. In the first step, the number of intrinsic impedance matrices is determined. In the second step, the number of mutual impedance matrices in the array is determined if unique matrices are determined.

5. Analysis of the spectral characteristics of the impedance matrix for a single spiral element

As shown above, the spiral geometry (Fig. 1, b) can be defined by six parameters: the lower and upper radii $r_{\max}$ and $r_{\min}$, the spiral height H, the winding direction s, the number of turns N_l, and the spiral conductor radius ε. For the given parameters, we can estimate the coefficients h_r and h_z (15) included in the spiral equation (14). To study the spectral character-

istics of the impedance matrix for a single spiral element, the use of normalized parameters is reasonable. The main parameter normalized to the wavelength λ should be the doubled maximum radius of the spiral $2r_{\max}$ (the maximum extent of a single element at $H < 2r_{\max}$). Let us denote the relation $2r_{\max}/\lambda$ as ς. For numerical simulations, we studied the spiral with the following parameters: $2r_{\min}/(2r_{\max}) = 0,3682$, $H/(2r_{\max}) = 0,025$, $\varepsilon/(2r_{\max}) = 0,0037$, $N_l = 2$, and $s = 1$. In this case, $L/(2r_{\max}) \approx 4,323$ or $L/\lambda = \chi \approx 4,323\varsigma$. The latter expression is useful because antenna arrays similar to the considered one may feature three types of resonances: thin-wire, surface, and volume. Thin-wire resonances are predominantly defined by the length and shape of the conductor. They are high-q resonances and are most pronounced at half-integer values of χ not exceeding several units. Meanwhile, surface resonances are defined by the shape of the spiral element's support structure. Volume resonances are defined by the volume containing the spiral conductor. As a rule, the resonances of the latter two types have significantly lower q. They occur at multiples of the antenna array wavelength and do not exceed several units.

For numerical simulation, the parameter ς varied from $0,0125$ to $0,53$ at $\chi \in [0,054; 2,28]$. The impedance matrices were formed using the conventional collocation method, and the number of segments M was assumed to be 179, which at the given ratio $\varepsilon/(2r_{\max})$ satisfied condition (12). Hereinafter, the wave impedance of the medium W_m is assumed to be 120π ohms, which is true for vacuum or air. We also assume that the medium is nondissipative. Therefore, the expression $k = 2\pi/\lambda$ can be used to calculate the wave number.

Fig. 3 shows the curves $\xi'_n = \mathrm{Re}\,\xi_n$, $\xi''_n = \mathrm{sgn}(\mathrm{Im}(\xi_n))$ $\lg(1+|\mathrm{Im}(\xi_n)|)$ (a), and $-\lg|\xi_n|$ vs. χ (b). The index n indicates the curve number. The curves show that the EF versus frequency curves are resonant. There are four resonances in the considered range. These resonances can be categorized as thin-wire ones because they closely match the $n/2$ values. The curves show that the resonance for the first EF occurs at χ, slightly less than $1/2$, whereas the resonances for the subsequent EFs occur at χ, greater than $n/2$. The larger the value of n, the larger the upward deviation. This can be understood if we represent each EF as a superposition of a pair of traveling waves propa-

gating along the conductor in opposite directions. It becomes obvious that the phase velocity of these waves for $n = 1$ is less than the speed of light and greater than the speed of light for $n > 1$. The growth of the phase velocity, in turn, is associated with a more intense turn-to-turn interaction promoted by the growth of χ and the features of the higher-order EFs. Moreover, the q-value of the resonances drops rather quickly as n grows.

Fig. 4 shows the first four normalized EFs $\breve{\beta}_n(l/L)/\breve{\beta}_{n,\max}$, calculated at the resonance values χ. Apparently, the shape of the EFs is close to that in (19), but the total EF amplitude at $n > 1$ has a significant imaginary component. We can also note here the asymmetry of the EF curves, which increases with n. This asymmetry is caused by the shape of the spiral element. The amplitude distributions show that the EFs are predominantly a standing wave. The nonzero currents in the nodes at $n > 1$ indicate the insignificant share of the traveling wave component. The direction of propagation of this component along the conductor can be identified by the direction of the EF amplitude decrease.

The study of the spectral characteristics of the impedance matrix of a single spiral element allows us to confirm that PFS (19) can be used to estimate resonances in antenna array elements. Notably, however, this estimation is approximate as the resonance properties of an element in a sufficiently dense array may differ from the characteristics of a single element. In this case, we can expect changes in the q-values of the resonances and resonance frequency shifts.

6. Performance of the block matrix compression algorithm: iterative process convergence

The geometry of the single element given in the previous section was used for the numerical simulation of the antenna array. We assumed that all the elements L_{i_x, i_y} related to the single element L according to expression (17) had the same constant angle $\phi_{i_x, i_y} = \phi$. For the simulation, the angle was assumed to be 0. The antenna was excited by the PEMW W, and its EMF was expressed by expression (18). The amplitude of the electric field vector E_0 was assumed to be 1 V/m, the initial phase ψ_0 was 0°, the angle ϖ_0 was 0°, and the polarization angle was $\varpi_0 = 90$
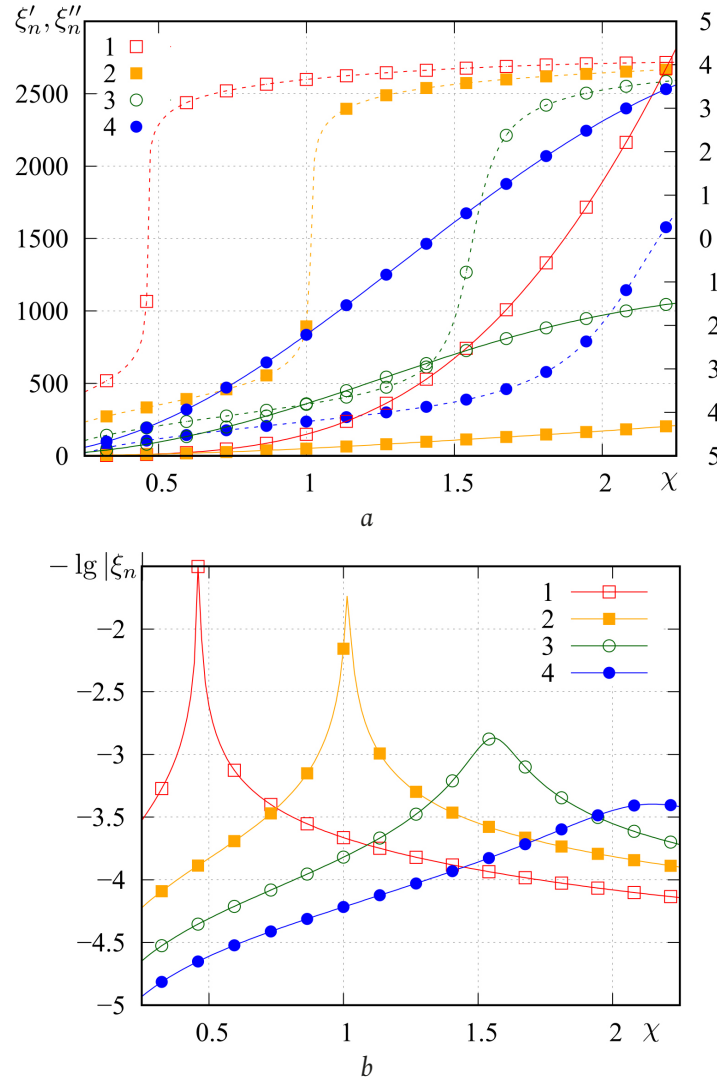
Fig. 3. Dependence $\xi'_n = \mathrm{Re}\,\xi_n$ (solid curves, *a*), $\xi''_n = \mathrm{sgn}(\mathrm{Im}(\xi_n))\,\lg(1+|\mathrm{Im}(\xi_n)|)$ (dashed curves, *a*) and $-\lg|\xi_n|$ (*b*) vs. χ. The curve number is the EV number

Рис. 3. Зависимость $\xi'_n = \mathrm{Re}\,\xi_n$ (сплошные кривые, *а*), $\xi''_n = \mathrm{sgn}(\mathrm{Im}(\xi_n))\,\lg(1+|\mathrm{Im}(\xi_n)|)$ (штриховые кривые, *а*) и $-\lg|\xi_n|$ (*б*) от χ; номер маркера (линии) соответствует номеру собственного значения

(H polarization). The incidence angles θ_0 were 0°, 45°, and 90°. We refer to these angles as the end, side, and normal PEMW incidences, respectively.

The array geometry is defined by four parameters: the distances between neighboring nodes h_x and h_y and the number of elements N_x, N_y along the coordinate axes. We denote the relation h_x/λ as ϑ. We assumed for the simulation that $h_x = h_y = h_a$, $N_x = N_y = N_a$. We considered antenna arrays with $N_a = 2, 4 \ldots 24$. The total number of elements N in such arrays was defined as N_a^2. For the considered array the parameters, ς and ϑ were related as $\varsigma/\vartheta = 0{,}53$, which was the fractional factor of the elements within the array. At $\varsigma/\vartheta = 1$, neighboring elements touched each other. We studied the range $\vartheta \in [0{,}0625; 1]$. In this case, the convergence of the iterative process

depended only on N_a and ϑ. Meanwhile, the compression ratio K/N depended only on N_a. Fig. 5 shows the compression ratio K/N against the number of the array N curve. Apparently, this relation is linear and can be approximated by the function $K/N \approx (4/15)N = (4/15)N_a^2$. Note that the direct calculation of the matrix elements produces a quadratic relation. The proposed algorithm for the calculation of the block matrix elements significantly reduces the required computer memory and computing time.

Fig. 6 shows the convergence table of the iterative process. The maximum number of iterations is 100. Reaching this value means no convergence. Considering the mentioned relation between σ and χ, thin-wire resonances in single elements of the array occurred at $\vartheta \approx 0{,}217n$, where n is the resonance
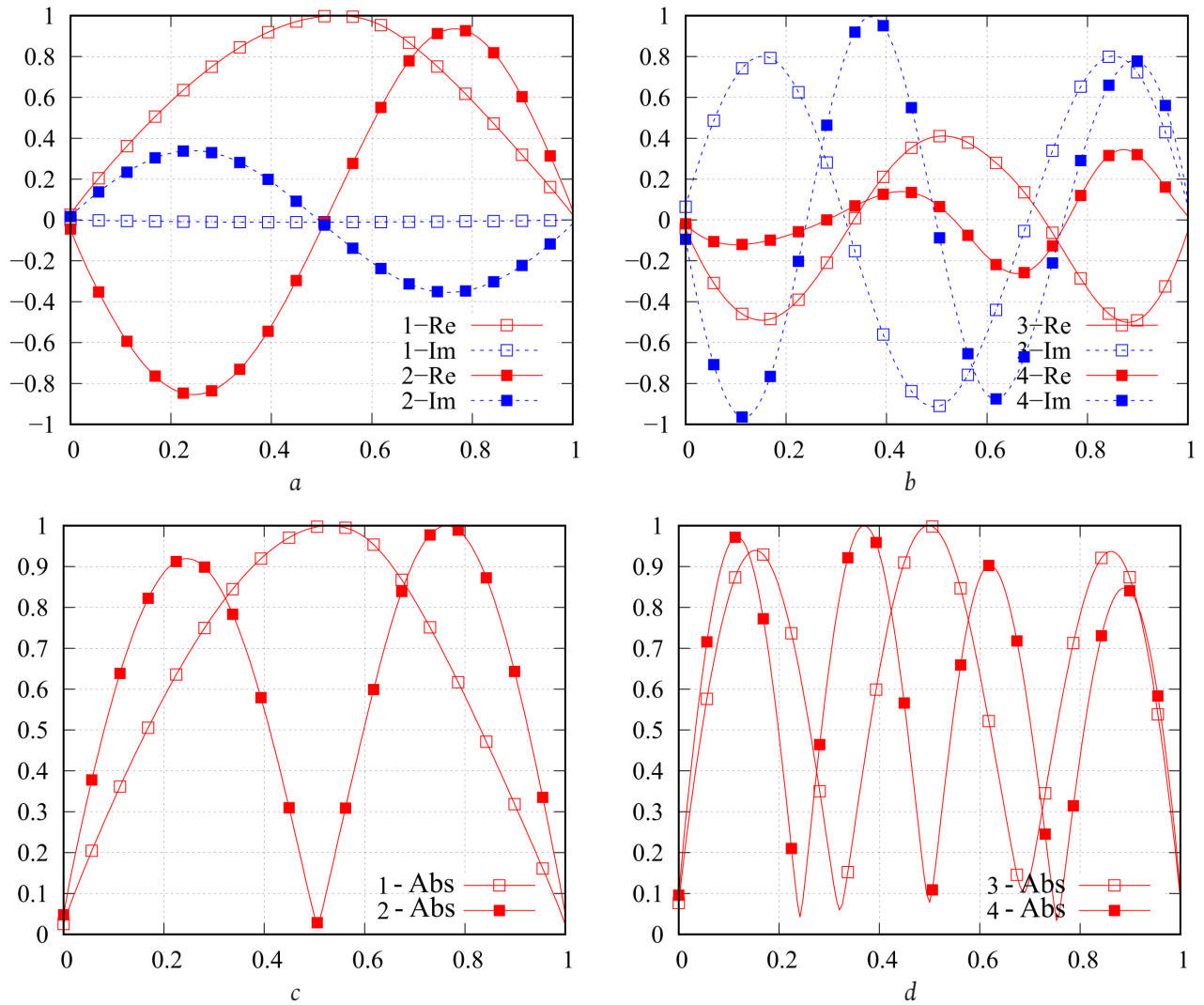
Fig. 4. First four normalized EFs $\bar{\beta}_n(l/L)/\bar{\beta}_{n,max}$, calculated at the corresponding resonance values χ. The numbers and components of the EFs are indicated on the curves

Рис. 4. Вид первых четырех нормированных собственных функций $\bar{\beta}_n(l/L)/\bar{\beta}_{n,max}$, вычисленных при соответствующих резонансных значениях χ; номера и составляющие собственных функций указаны на графиках
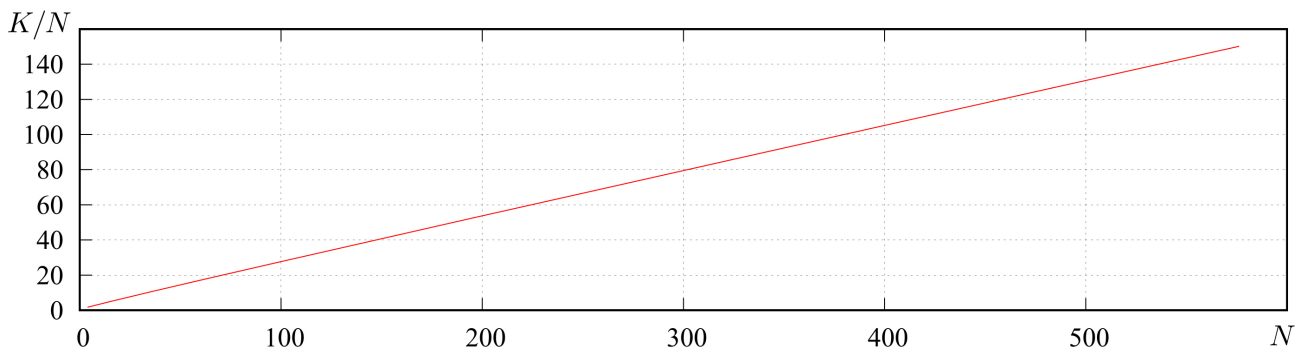

Fig. 5. Compression ratio K/N versus the number of array elements N

Рис. 5. Зависимость коэффициента сжатия K/N от числа элементов структуры N
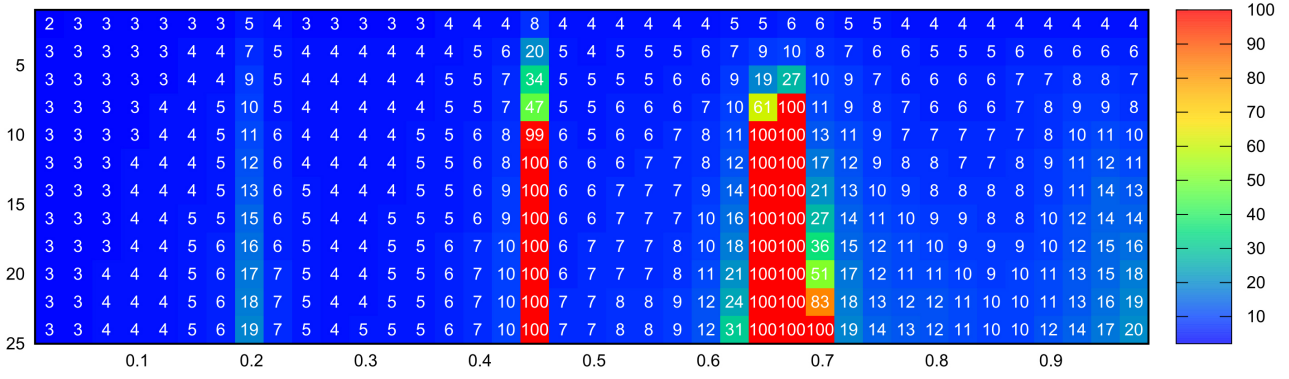
Fig. 6. Iterative process convergence table: abscissa axis is ϑ, ordinate axis is N_a, values in cells are number of iterations

Рис. 6. Таблица сходимости итерационного процесса: ось абсцисс – ϑ, ось ординат – N_a, значения в ячейках – число итераций

number. For the first four EFs, the resonances should occur in the neighborhood of $\vartheta = 0{,}217,\ 0{,}434,\ 0{,}651$, and $0{,}868$. The resonance frequencies could shift because of the interaction between the antenna array elements. The figure shows that the deterioration and lack of convergence occurred in the neighborhood of the resonance frequencies of the first three EFs. The first resonance did not lead to the loss of convergence, whereas the fourth EF resonance did not manifest itself. For a more complete explanation of this effect, we must analyze the angular distributions of each EF field and determine the spatial orientations of the field maxima.

7. Analysis and interpretation of the proposed internal electrodynamic problem

Let us consider the external field functions and current distribution functions approximated by the expansions in the EFs of the single element's integral operator (2):

$$\eta_n(l) = \sum_q I_q^{(n)} \breve{\beta}_{n,q}(l), \quad \zeta_n(l) = \sum_q E_q^{(n)} \breve{\beta}_{n,q}(l);$$

$$l \in L, \quad I_q^{(n)} \in \mathbf{i}_n, \quad E_q^{(n)} \in \mathbf{e}_n.$$

For the considered array, the vectors of the amplitude coefficients averaged over n can be reasonably used:

$$\dot{\mathbf{f}}^{(a)} \supset \dot{F}_q^{(a)}, \quad \dot{F}_q^{(a)} = \frac{1}{N}\sum_n |F_q^{(n)}|, \quad \mathbf{f} \equiv \mathbf{i}, \mathbf{e},\ F \equiv I, E,$$

The corresponding mismatch values $\rho_n^{(\mathbf{f},a)} = |\dot{\mathbf{f}}^{(a)} - \mathbf{f}_n^{(a)}| / |\dot{\mathbf{f}}^{(a)}|;\quad \mathbf{f} \equiv \mathbf{i}, \mathbf{e}$. The simulation indicated that in the studied frequency range for the arrays with $N_a = 2\ldots24$ at $\theta_0 = 0\ldots90°$ angles of incidence,

the average values of these mismatches did not exceed $0{,}09$ and the median values were less than $0{,}025$. Meanwhile, it confirmed the applicability of the averaged vectors of the amplitude coefficients and indicated a high homogeneity of the current distribution functions. Hereinafter, the vectors of the amplitude coefficients normalized to the maximum value are denoted as $\mathbf{f}^{(a/\max)} = \mathbf{f}^{(a)} / f_{\max}^{(a)}$. $f_{\max}^{(a)}$ is the maximum amplitude element of the vector $\mathbf{f}$, and $f_{\mathrm{nrm}}^{(a)} = |\mathbf{f}^{(a)}|$ is its Euclidean norm. The supremum of the vector $\mathbf{f}^{(a)}$ is the value $f^{(\sup)} = \max(f_{\max}^{(a)}, f_{\mathrm{nrm}}^{(a)})$.

Fig. 7 (top) shows the normalized spectrogram $\dot{\mathbf{e}}^{(a/\max)}(\vartheta)$ for $N_a = 8$, $\theta_0 = 90°$. The abscissa axis indicates the ϑ values, whereas the ordinate axis indicates the number of vector elements $\dot{\mathbf{e}}^{(a/\max)}$. Apparently, the spectrogram shape did not depend on ϑ, and the maximum amplitude corresponded to the fourth EF. This was because the spiral elements had two turns. In general, we can note that the spectrum was quite broad in the range ϑ. Fig. 7 (bottom) shows the normalized spectrogram $\mathbf{i}^{(a/\max)}(\vartheta)$ for a similar case, and Fig. 8 shows the $\dot{f}_j^{(a/\sup)} = \dot{f}_j^{(a)}(\vartheta) / \dot{f}^{(\sup)}$ ($f \equiv i, e,\ j \equiv \max, \mathrm{nrm}$) curves. These relations and the spectrogram indicate that the spectrum of the EFs of the antenna array in the investigated range θ is narrowband and resonant.

The difference in the amplitudes of the curves $\dot{f}_{\max}^{(a/\sup)}$ and $\dot{f}_{\mathrm{nrm}}^{(a/\sup)}$ ($f \equiv i, e$) can be used to estimate the spectrum degeneracy. If $\dot{f}_{\max}^{(a/\sup)} = \dot{f}_{\mathrm{nrm}}^{(a/\sup)}$, then the spectrum is degenerate and consists of only one spectral component. The external field spectrum was nondegenerate over the entire range, whereas the spectrum of the current functions was close to degenerate and was virtually degenerate near the resonance frequencies of the antenna array element EVs.
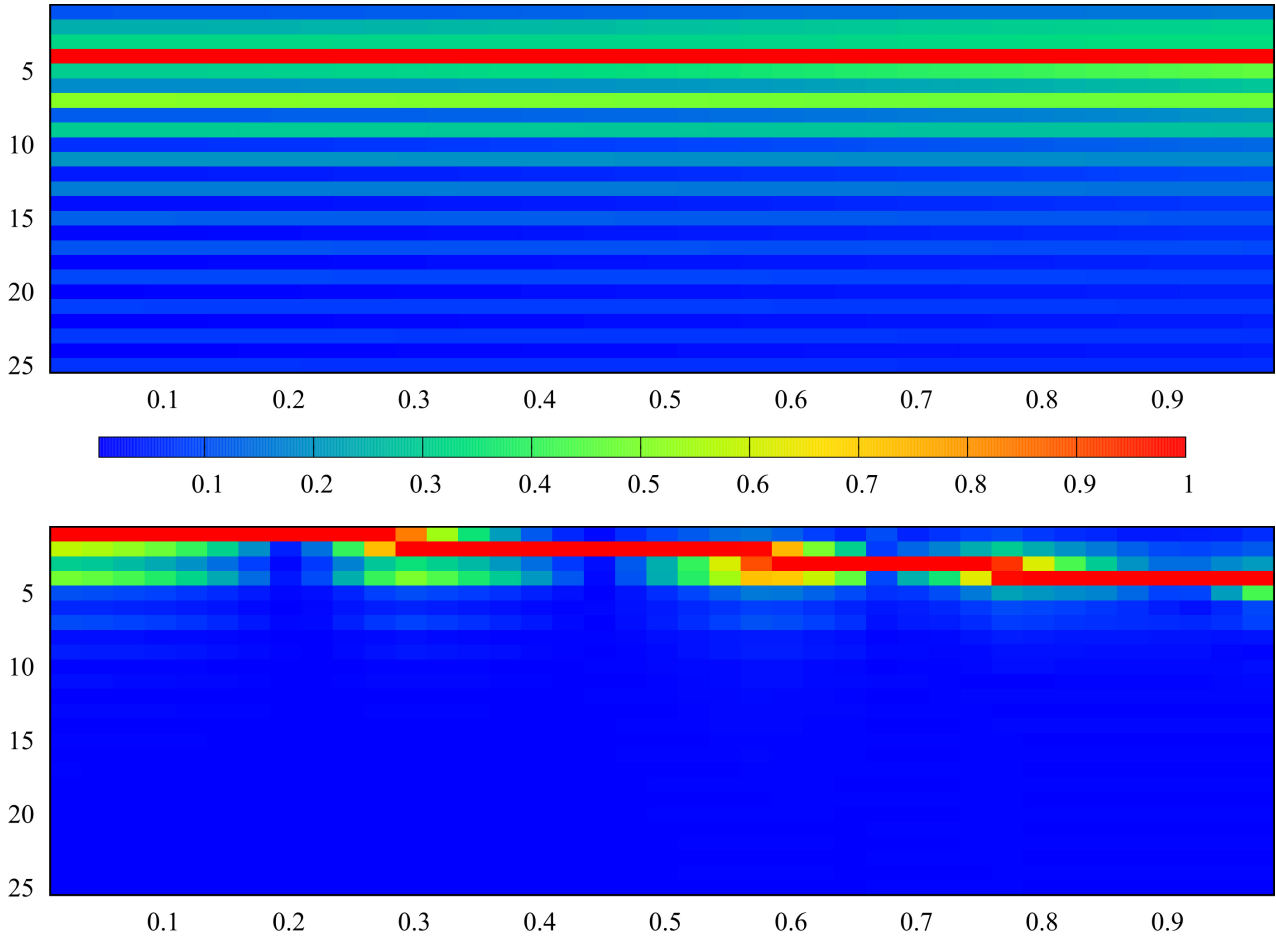
Fig. 7. Spectrograms: top – $\dot{\mathbf{e}}^{(a/\max)}(\vartheta)$, bottom – $\dot{\mathbf{i}}^{(a/\max)}(\vartheta)$; abscissa axis – ϑ, ordinate axis – index of the vector element
Рис. 7. Спектрограммы: сверху – $\dot{\mathbf{e}}^{(a/\max)}(\vartheta)$, снизу – $\dot{\mathbf{i}}^{(a/\max)}(\vartheta)$; ось абсцисс – ϑ, ось ординат – индекс элемента векторов
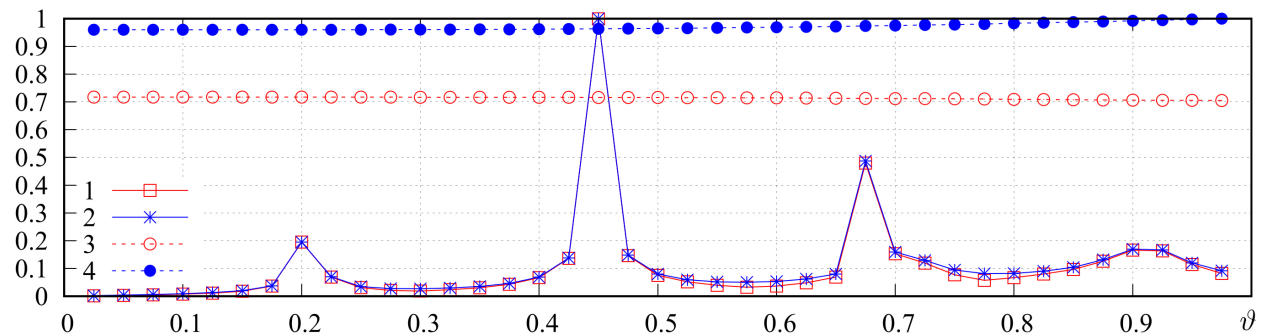
Fig. 8. Dependencies $\dot{i}_{\max}^{(a/\sup)}$ (curve 1), $\dot{i}_{\mathrm{nrm}}^{(a/\sup)}$ (curve 2), $\dot{e}_{\max}^{(a/\sup)}$ (curve 3), and $\dot{e}_{\mathrm{nrm}}^{(a/\sup)}$ (curve 4) vs. ϑ
Рис. 8. Зависимости $\dot{i}_{\max}^{(a/\sup)}$ (кривая 1), $\dot{i}_{\mathrm{nrm}}^{(a/\sup)}$ (кривая 2), $\dot{e}_{\max}^{(a/\sup)}$ (кривая 3) и $\dot{e}_{\mathrm{nrm}}^{(a/\sup)}$ (кривая 4) от ϑ

The above results are crucial for metastructure analyses because they allow us to use a compact set of EFs with significant amplitudes in the neighborhood of the considered frequency as projection functions. For finite-size arrays, the SLAE can be solved directly. The SLAE has the smallest matrix size at the resonant frequencies when the current distribution over the elements is determined by only one EF (degen-erate current distributions). In this case, finding the EVECs of the antenna array that define a finite set of distributions of the complex amplitudes of the degenerate current distributions on the array elements is beneficial. The authors aim to solve this problem and determine the characteristics of the scattered field for the considered array in resonant and non-resonant cases.

Conclusion

This study presented a systematic approach to the rigorous solution to the internal electrodynamic problem for multielement antenna arrays. The approach was based on the Gauss–Seidel or Jacobi-type iterative procedures applied to the block matrix of the SLAE obtained using the method of moments [15]. This approach implied the use of a priori information about the array to implement efficient algorithms for the analysis of the SLAE block matrix [18]. Moreover, this study showed the feasibility of determining the spectral characteristics of the integral operators of the internal problem for single elements that are part of the antenna array. The solution resulted in the determination of the EFs and EVs of the integral operators and their frequency dependence. The identification of EFs allowed us to reasonably select the systems of projection functions used in the method of moments to generate the SALE block. The EV versus frequency relationship allowed us to predict the resonances in multielement arrays.

This paper demonstrated the application of the proposed approach to solving the intrinsic problem for a specific regular 2D array consisting of conical spiral elements excited by a plane linearly polarized electromagnetic wave. We also identified the relationship between the frequency dependence of the integral operator's EV numbers determined for a single array element and the resonances occurring in the array and confirmed the relationship between the resonances and the convergence of the iterative process. We studied the spectra of the current distribution functions for the array elements. The amplitude spectra at different elements of the array were very similar, so the averaged amplitude spectra can be used in the analysis. We found that the averaged spectrum of the external field at the array elements was relatively broad, whereas the averaged spectrum of the current distribution functions was close to degenerate and was virtually degenerate near the resonant frequencies. These features allowed us to use a compact set of EFs with significant amplitudes in the vicinity of the studied frequency as projection functions. It ultimately led to a reduction in the SLAE matrix block sizes and significantly simplified the solution to the internal problem.

The presented results once again confirm the efficiency of the iterative approach to the rigorous solution to the internal electrodynamic problem for multielement arrays in nonresonant cases. The authors propose introducing resonance identification procedures. The internal problem in the neighborhood of resonance frequencies requires special attention.

References

1. V. A. Neganov and O. V. Osipov, Reflective, *Waveguide and Radiating Structures with Chiral Elements*. Moscow: Radio i svyaz', 2006. (In Russ.)

2. E. L. Ivchenko and A. N. Poddubnyy, "Resonant three-dimensional photonic crystals," *Fizika tverdogo tela*, vol. 48, no. 3, pp. 540–547, 2006, url: https://journals.ioffe.ru/articles/3354. (In Russ.)

3. V. G. Veselago, "Electrodynamics of substances with simultaneously negative values of ε and μ," *Uspekhi fizicheskikh nauk*, vol. 92, no. 3, pp. 517–526, 1967, doi: https://doi.org/10.3367/UFNr.0092.196707d.0517. (In Russ.)

4. J. B. Pendry, "A chiral route to negative refraction," *Science*, vol. 306, no. 5700, pp. 1353–1355, 2004, doi: https://doi.org/10.1126/science.1104467.

5. D. R. Smith et al., "Composite medium with simultaneously negative permeability and permittivity," *Physical Review Letters*, vol. 84, no. 18, pp. 4184–4187, 2000, doi: https://doi.org/10.1103/PhysRevLett.84.4184.

6. J. B. Pendry et al., "Extremely low frequency plasmons in metallic mesostructures," *Physical Review Letters*, vol. 76, no. 25, pp. 4773–4776, 1996, doi: https://doi.org/10.1103/PhysRevLett.76.4773.

7. J. B. Pendry et al., "Low frequency plasmons in thin-wire structures," *Journal of Physics: Condensed Matter*, vol. 10, no. 22, pp. 4785–4809, 1998, doi: https://doi.org/10.1088/0953-8984/10/22/007.

8. J. B. Pendry et al., "Magnetism from conductors and enhanced nonlinear phenomena," *IEEE Transactions on Microwave Theory and Techniques*, vol. 47, no. 11, pp. 2075–2084, 1999, doi: https://doi.org/10.1109/22.798002.

9. I. B. Vendik and O. G. Vendik, "Metamaterials and their application in microwave technology (Review)," *Zhurnal tekhnicheskoy fiziki*, vol. 83, no. 1, pp. 3–28, 2013, url: https://journals.ioffe.ru/articles/viewPDF/41403. (In Russ.)

10. S. A. Schelkunoff and H. T. Friis, *Antennas Theory and Practice*. New York: Wiley, 1952.

11. R. F. Harrington, *Field Computation by Moment Method*. New York: Macmillan, 1968.

12. R. H. Gallagher, *Finite Element Analysis: Fundamentals*. Hoboken: Prentice-Hall, 1974.

13. V. N. Kisel' and A. N. Lagar'kov, "Electrodynamic models of thin-layer metamaterials and devices based on them," *Radiotekhnika i elektronika*, vol. 54, no. 5, pp. 531–540, 2009, url: https://elibrary.ru/item.asp?id=12136589. (In Russ.)

14. A. S. Il'inskiy, O. Yu. Perfilov, and A. B. Samokhin, "Iterative method for solving integral equations of the theory of wire antennas," *Matematicheskoe modelirovanie*, vol. 6, no. 3, pp. 52–59, 1994, url: https://www.mathnet.ru/rus/mm1848. (In Russ.)

15. V. A. Neganov, I. Yu. Marsakov, and D. P. Tabakov, "The calculation of the interaction of elements metastructures based on the Gauss–Seidel method," *Physics of Wave Processes and Radio Systems*, vol. 16, no. 3, pp. 6–16, 2013, url: https://elibrary.ru/item.asp?id=21007651. (In Russ.)

16. N. S. Bakhvalov, N. P. Zhidkov, and G. M. Kobel'kov, *Numerical Methods*. Moscow: Laboratoriya bazovykh znaniy, 2000. (In Russ.)

17. V. A. Neganov and D. P. Tabakov, "Correct electrodynamic analysis of chiral elements and metamaterials based on integral representations of the electromagnetic field," *Physics of Wave Processes and Radio Systems*, vol. 17, no. 3, pp. 29–39, 2014, url: https://journals.ssau.ru/pwp/article/view/7265. (In Russ.)

18. D. P. Tabakov, "Application of iterative procedures to electrodynamic analysis of metamaterials," *Radiotekhnika*, no. 7, pp. 86–94, 2015, url: https://elibrary.ru/item.asp?id=23837442. (In Russ.)

19. D. P. Tabakov and B. M. A. Al-Nozaili, "Calculation of currents on multi-element radiating structures using the iterative method," *Radiotekhnika i elektronika*, vol. 67, no. 7, pp. 651–659, 2022, url: https://elibrary.ru/item.asp?id=48867815. (In Russ.)

20. A. L. Drabkin, V. L. Zuzenko, and A. G. Kislov, *Antenna-Feeder Devices*, 2nd ed., add. and rework. Moscow: Sov. radio, 1974. (In Russ.)

21. D. P. Tabakov and B. M. A. Al-Nozaili, "Solution of the internal and external problems of electrodynamics for a symmetrical vibrator with a reflector made of parallel straight conductors," *Physics of Wave Processes and Radio Systems*, vol. 27, no. 2, pp. 7–21, 2024, doi: https://doi.org/10.18469/1810-3189.2024.27.2.7-21. (In Russ.)

22. D. P. Tabakov, "On the description of radiation and diffraction of electromagnetic waves by the method of eigenfunctions," *Izvestiya vuzov. Radiofizika*, vol. 64, no. 3, pp. 179–191, 2021, url: https://radiophysics.unn.ru/issues/2021/3/179. (In Russ.)

23. D. P. Tabakov and A. G. Mayorov, "Approximation of the solution to the internal electrodynamic problem for a thin tubular vibrator using the eigenfunction method," *Trudy uchebnykh zavedeniy svyazi*, vol. 5, no. 4, pp. 58–64, 2019, doi: https://doi.org/10.31854/1813-324X-2019-5-4-58-64. (In Russ.)

24. V. A. Kapitonov et al., "Integral representation of the electromagnetic field of geometrically chiral structure," *Physics of Wave Processes and Radio Systems*, vol. 15, no. 4, pp. 6–13, 2012, url: https://www.elibrary.ru/item.asp?id=19001844. (In Russ.)

25. R. Mittra, Ed. *Computational Methods in Electrodynamics*; transl. E. L. Burshteyn, Ed. Moscow: Mir, 1977. (In Russ.)

26. V. A. Strizhkov, "Mathematical modeling of electrodynamic processes in complex antenna systems," *Matematicheskoe modelirovanie*, vol. 1, no. 8, pp. 127–138, 1989, url: https://www.mathnet.ru/rus/mm2614. (In Russ.)

Information about the Authors

Dmitry P. Tabakov, Doctor of Physical and Mathematical Sciences, professor of the Department of Radioelectronic Systems, Povolzhskiy State University of Telecommunications and Informatics, Samara, Russia.

Research interests: electrodynamics, microwave devices and antennas, optics, numerical methods of mathematical modeling.

E-mail: illuminator84@yandex.ru

ORCID: https://orcid.org/0000-0002-9173-4936

SPIN-code (eLibrary): 9666-0814

AuthorID (eLibrary): 664833

ResearcherID (WoS): Q-9888-2017

Bassam Mohammed-Ali Al-Nozaili, graduate student of Samara National Research University, assistant professor of the Department of Physics, Povolzhskiy State University of Telecommunications and Informatics, Samara, Russia.

Research interests: electrodynamics, microwave devices and antennas.

E-mail: bassam_91@mail.ru

SPIN-code (eLibrary): 7368-7223

AuthorID (eLibrary): 1204671

Решение внутренней задачи для конечной регулярной двумерной решетки спиральных элементов, возбуждаемой плоской электромагнитной волной

Д.П. Табаков[1] 🆔 *, Б.М.А. Аль-Нозайли*[2]

[1] Поволжский государственный университет телекоммуникаций и информатики
443010, Россия, г. Самара,
ул. Л. Толстого, 23
[2] Самарский национальный исследовательский университет имени академика С.П. Королева
443086, Россия, г. Самара,
Московское шоссе, 34

Аннотация – **Обоснование.** Работа направлена на развитие и исследование строгих методов решения внутренней задачи электродинамики для многоэлементных структур (метаструктур), состоящих из конечного числа элементов, а также на исследование протекающих в них физических процессов. Частным случаем подобных структур являются двумерные решетки с фиксированным межэлементным расстоянием, состоящие из одинаковых элементов, имеющих одну и ту же пространственную ориентацию (регулярные решетки). **Цель.** На основе итерационного подхода осуществляется решение внутренней задачи электродинамики для конечной регулярной двумерной решетки спиральных элементов. С целью получения априорной информации об электродинамических характеристиках элементов решетки и обоснования выбора систем проекционных функций осуществляется анализ спектральных характеристик интегрального оператора внутренней задачи для одиночного спирального элемента. Затем производится расчет токов на элементах структуры, определяются их спектральные характеристики. Результаты спектрального анализа позволяют повысить эффективность решения внутренней задачи. **Методы.** В основе исследований лежит строгий электродинамический подход, в рамках которого для указанной структуры в тонкопроволочном приближении формируется интегральное представление электромагнитного поля, сводящееся при рассмотрении на поверхности проводников совместно с граничными условиями к системе интегральных уравнений Фредгольма второго рода, записанных относительно неизвестных распределений тока на проводниках (внутренняя задача). Решение внутренней задачи в рамках метода моментов сводится к решению СЛАУ с блочной матрицей. **Результаты.** Предложена математическая модель конечной двумерной решетки спиральных элементов излучающей структуры. Для указанной структуры в случае ее возбуждения плоской электромагнитной волной на основе итерационного подхода решена внутренняя задача электродинамики. В широкой полосе частот проведены: анализ сходимости итерационного процесса, спектральный анализ интегрального оператора внутренней задачи для одиночного спирального элемента, а также спектральный анализ функций стороннего поля и токовых функций на элементах решетки. **Заключение.** Показана целесообразность определения спектральных характеристик интегральных операторов внутренней задачи для элементов, образующих метаструктуру. Выявлена связь между частотной зависимостью собственных чисел интегрального оператора внутренней задачи одиночных элементов, образующих метаструктуру, с резонансными явлениями, возникающими в метаструктуре, подтверждено влияние резонансов на сходимость итерационного процесса. Показана целесообразность рассмотрения усредненных амплитудных токовых спектров. Выявлено, что усредненный спектр токовых функций близок к вырожденному, особенно вблизи резонансных частот. Это позволяет использовать в качестве проекционных функций компактный набор собственных функций, имеющих существенные амплитуды в окрестности исследуемой частоты, что существенно упрощает решение внутренней задачи.

Ключевые слова – метаструктура; спиральная структура; интегральное уравнение Фредгольма; тонкопроволочное приближение; интегральное представление электромагнитного поля; резонанс; распределение тока; метод Гаусса – Зейделя; метод собственных функций.

Список литературы

1. Неганов В.А., Осипов О.В. Отражающие, волноведущие и излучающие структуры с киральными элементами. М.: Радио и связь, 2006. 280 с.

2. Ивченко Е.Л., Поддубный А.Н. Резонансные трехмерные фотонные кристаллы // Физика твердого тела. 2006. Т. 48, № 3. С. 540–547. URL: https://journals.ioffe.ru/articles/3354

3. Веселаго В.Г. Электродинамика веществ с одновременно отрицательными значениями ε и μ // Успехи физических наук. 1967. Т. 92, № 3. С. 517–526. DOI: https://doi.org/10.3367/UFNr.0092.196707d.0517

4. Pendry J.B. A chiral route to negative refraction // Science. 2004. Vol. 306, no. 5700. P. 1353–1355. DOI: https://doi.org/10.1126/science.1104467

Tabakov D.P., Bassam Mohammed-Ali Al-Nozaili Solving an internal problem for finite regular two-dimensional lattice ...

32   Табаков Д.П., Аль-Нозайли Б.М.А. Решение внутренней задачи для конечной регулярной двумерной решетки ...

5. Composite medium with simultaneously negative permeability and permittivity / D.R. Smith [et al.] // Physical Review Letters. 2000. Vol. 84, no. 18. P. 4184–4187. DOI: https://doi.org/10.1103/PhysRevLett.84.4184

6. Extremely low frequency plasmons in metallic mesostructures / J.B. Pendry [et al.] // Physical Review Letters. 1996. Vol. 76, no. 25. P. 4773–4776. DOI: https://doi.org/10.1103/PhysRevLett.76.4773

7. Low frequency plasmons in thin-wire structures / J.B. Pendry [et al.] // Journal of Physics: Condensed Matter. 1998. Vol. 10, no. 22. P. 4785–4809. DOI: https://doi.org/10.1088/0953-8984/10/22/007

8. Magnetism from conductors and enhanced nonlinear phenomena / J.B. Pendry [et al.] // IEEE Transactions on Microwave Theory and Techniques. 1999. Vol. 47, no. 11. P. 2075–2084. DOI: https://doi.org/10.1109/22.798002

9. Вендик И.Б., Вендик О.Г. Метаматериалы и их применение в технике сверхвысоких частот (Обзор) // Журнал технической физики. 2013. Т. 83, № 1. С. 3–28. URL: https://journals.ioffe.ru/articles/viewPDF/41403

10. Schelkunoff S.A., Friis H.T. Antennas Theory and Practice. New York: Wiley, 1952. 672 p.

11. Harrington R.F. Field Computation by Moment Method. New York: Macmillan, 1968. 150 p.

12. Gallagher R.H. Finite Element Analysis: Fundamentals. Hoboken: Prentice-Hall, 1974. 420 p.

13. Кисель В.Н., Лагарьков А.Н. Электродинамические модели тонкослойных метаматериалов и устройства на их основе // Радиотехника и электроника. 2009. Т. 54. № 5. С. 531–540. URL: https://elibrary.ru/item.asp?id=12136589

14. Ильинский А.С., Перфилов О.Ю., Самохин А.Б. Итерационный метод решения интегральных уравнений теории проволочных антенн // Математическое моделирование. 1994. Т. 6, № 3. С. 52–59. URL: https://www.mathnet.ru/rus/mm1848

15. Неганов В.А., Марсаков И.Ю., Табаков Д.П. Расчет взаимодействия элементов метаструктуры на основе метода Гаусса – Зейделя // Физика волновых процессов и радиотехнические системы. 2013. Т. 16, № 3. С. 6–16. URL: https://elibrary.ru/item.asp?id=21007651

16. Бахвалов Н.С., Жидков Н.П., Кобельков Г.М. Численные методы. М.: Лаборатория базовых знаний, 2000. 624 с.

17. Неганов В.А., Табаков Д.П. Корректный электродинамический анализ киральных элементов и метаматериалов на основе интегральных представлений электромагнитного поля // Физика волновых процессов и радиотехнические системы. 2014. Т. 17, № 3. С. 29–39. URL: https://journals.ssau.ru/pwp/article/view/7265.

18. Табаков Д.П. Применение итерационных процедур к электродинамическому анализу метаматериалов // Радиотехника. 2015. № 7. С. 86–94. URL: https://elibrary.ru/item.asp?id=23837442

19. Табаков Д.П., Аль-Нозайли Б.М.А. Расчет токов на многоэлементных излучающих структурах итерационным методом // Радиотехника и электроника. 2022. Т. 67, № 7. С. 651–659. URL: https://elibrary.ru/item.asp?id=48867815

20. Драбкин А.Л., Зузенко В.Л., Кислов А.Г. Антенно-фидерные устройства. 2-е изд., доп. и перераб. М.: Сов. радио, 1974. 536 с.

21. Табаков Д.П., Аль-Нозайли Б.М.А. Решение внутренней и внешней задач электродинамики для симметричного вибратора с рефлектором из параллельных прямолинейных проводников // Физика волновых процессов и радиотехнические системы. 2024. Т. 27, № 2. С. 7–21. DOI: https://doi.org/10.18469/1810-3189.2024.27.2.7-21

22. Табаков Д.П. Об описании излучения и дифракции электромагнитных волн методом собственных функций // Известия вузов. Радиофизика. 2021. Т. 64, № 3. С. 179–191. URL: https://radiophysics.unn.ru/issues/2021/3/179

23. Табаков Д.П., Майоров А.Г. Аппроксимация решения внутренней электродинамической задачи для тонкого трубчатого вибратора методом собственных функций // Труды учебных заведений связи. 2019. Т. 5, № 4. С. 58–64. DOI: https://doi.org/10.31854/1813-324X-2019-5-4-58-64

24. Интегральное представление электромагнитного поля геометрически киральной структуры / В.А. Капитонов [и др.] // Физика волновых процессов и радиотехнические системы. 2012. Т. 15, № 4. С. 6–13. URL: https://www.elibrary.ru/item.asp?id=19001844

25. Вычислительные методы в электродинамике / под ред. Р. Митры; пер с англ. под ред. Э.Л. Бурштейна. М.: Мир, 1977. 487 с.

26. Стрижков В.А. Математическое моделирование электродинамических процессов в сложных антенных системах // Математическое моделирование. 1989. Т. 1, № 8. С. 127–138. URL: https://www.mathnet.ru/rus/mm2614

Информация об авторах

Табаков Дмитрий Петрович, доктор физико-математических наук, профессор кафедры физики Поволжского государственного университета телекоммуникаций и информатики, г. Самара, Россия.

Область научных интересов: электродинамика, устройства СВЧ и антенны, оптика, численные методы математического моделирования.

E-mail: illuminator84@yandex.ru

ORCID: https://orcid.org/0000-0002-9173-4936

SPIN-код (eLibrary): 9666-0814

AuthorID (eLibrary): 664833

ResearcherID (WoS): Q-9888-2017